



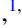


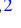




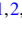

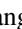





Pressure-induced dependence of transport properties and lattice stability of $\text{CaK}(\text{Fe}_{1-x}\text{Ni}_x)_4\text{As}_4$ ($x = 0.04$ and 0) superconductors with and without a spin-vortex crystal state

Pengyu Wang ^{1,2,*}, Chang Liu ^{1,2,*}, Run Yang ^{1,*}, Shu Cai ^{1,3}, Tao Xie ^{1,2}, Jing Guo ^{1,5}, Jinyu Zhao ^{1,2}, Jinyu Han ^{1,2}, Sijin Long ^{1,2}, Yazhou Zhou ¹, Yanchun Li ³, Xiaodong Li ³, Huiqian Luo ^{1,2,5}, Shiliang Li ^{1,2,5}, Qi Wu ¹, Xianggang Qiu ^{1,2,5}, Tao Xiang ^{1,2} and Liling Sun ^{1,2,3,5,†}

¹*Institute of Physics, Chinese Academy of Sciences, Beijing 100190, China*

²*University of Chinese Academy of Sciences, Beijing 100190, China*

³*Center for High Pressure Science & Technology Advanced Research, 100094 Beijing, China*

⁴*Institute of High Energy Physics, Chinese Academy of Science, Beijing 100049, China*

⁵*Songshan Lake Materials Laboratory, Dongguan, Guangdong 523808, China*



(Received 13 January 2023; revised 24 June 2023; accepted 19 July 2023; published 9 August 2023)

Here we report the investigation on correlation between the transport properties and the corresponding stability of the lattice structure for $\text{CaK}(\text{Fe}_{1-x}\text{Ni}_x)_4\text{As}_4$ ($x = 0.04$ and 0), a new type of putative topological superconductors with and without a spin-vortex crystal (SVC) state in a wide pressure range involving superconducting (SC) to nonsuperconducting (NSC) transition and the half to full collapse of tetragonal [half-collapsed tetragonal (h-cT) and full-collapsed tetragonal (f-cT)] phases by the complementary measurements of high-pressure resistance, Hall coefficient, and synchrotron x-ray diffraction. The three critical pressures are identified: P_{ch}^{on} that is the turn-on critical pressure of the h-cT phase transition and it coincides with the critical pressure for the sign change of Hall coefficient from positive to negative, a manifestation of the Fermi surface reconstruction; P_{ch}^{off} that is the turn-off pressure of the h-cT phase transition; and P_{cf} that is the critical pressure of the f-cT phase transition. By comparing the high-pressure results measured from the two kinds of samples, we find a distinct “left-shift” of the P_{ch}^{on} for the doped sample, at the pressure of which its SVC state is fully suppressed, however, the P_{ch}^{off} and the P_{cf} remain the same as that of the undoped one. Our results not only provide a consistent understanding on the results reported before, but also demonstrate the importance of the Fe-As bonding in stabilizing the superconductivity of the iron pnictide superconductors through the “pressure window.”

DOI: [10.1103/PhysRevB.108.054415](https://doi.org/10.1103/PhysRevB.108.054415)

The discovery of the high- T_c iron-pnictide and iron-selenide superconductors [1,2] provides a new platform to specify the essential ingredients existed in cuprate superconductors, and an opportunity to achieve a better understanding on the mechanism of high- T_c superconductivity, a “holy grail” in the field of the contemporary condensed-matter physics and material sciences [3–5]. Now, several types of iron-pnictide superconductors have been found [6–9], all of which have the tetrahedra structure with the Fe-As layers stacking alternatively with other intermediary layers/atoms. Growing evidence from experiments indicates that the Fe-As layers play a key role in developing and stabilizing superconductivity [9]. In 2016, a new member of the iron pnictide superconductors, $\text{AeAFe}_4\text{As}_4$ ($\text{Ae} = \text{Ca}, \text{Sr}$ and $A = \text{K}, \text{Rb}$, and Cs), has been found [10–26]. Structurally, it can be regarded as the hybrid phases between AeFe_2As_2 and AFe_2As_2 with the stoichiometric composition, whereas, is different from most of the other known high- T_c superconductors whose superconductivity are induced by chemical doping. As a result, these stoichiometric superconductors have no chem-

ical substitution-induced inhomogeneity on the lattice, and significantly reduced the complexity of the local structure for understanding the physics behind. Since the Ae^{2+} and A^{1+} atoms are inserted alternately across the Fe_2As_2 layers, the $\text{AeAFe}_4\text{As}_4$ superconductors host two different sites of As ions in a unit cell [As(1) and As(2), respectively] in the tetragonal unit cell with space-group $P4/mmm$ [10]. Upon cooling, they show a superconducting transition at the temperature (T_c) varying from 31 to 36 K. Partial substituting Fe with Ni, Co, or Mn reduces the T_c value by more than 10 K due to the existence of a spin-vortex crystal (SVC) state with Fe spins lying in plane and stacking along the c axis antiferromagnetically that competes with the superconducting (SC) state [22–24]. Remarkably, recent angle-resolved photoemission spectroscopy and scanning tunneling microscopy/spectroscopy experiments find the evidence of the Dirac surface state and Majorana zero mode in the $\text{CaKFe}_4\text{As}_4$ superconductor [21], implying that this type of superconductors may host some nontrivial quantum states, such as topological superconductivity. Moreover, inelastic neutron-scattering experiments find that the spin resonance of the $\text{CaK}(\text{Fe}_{1-x}\text{Ni}_x)_4\text{As}_4$ superconductor displays both odd and even modes along the L direction [17,18], similar to the resonance observed in bilayer cuprate superconductors [27]. These findings attract additional research interest on them.

*These authors contributed equally to this work

†Correspondence and requests for materials should be addressed to llsun@iphy.ac.cn

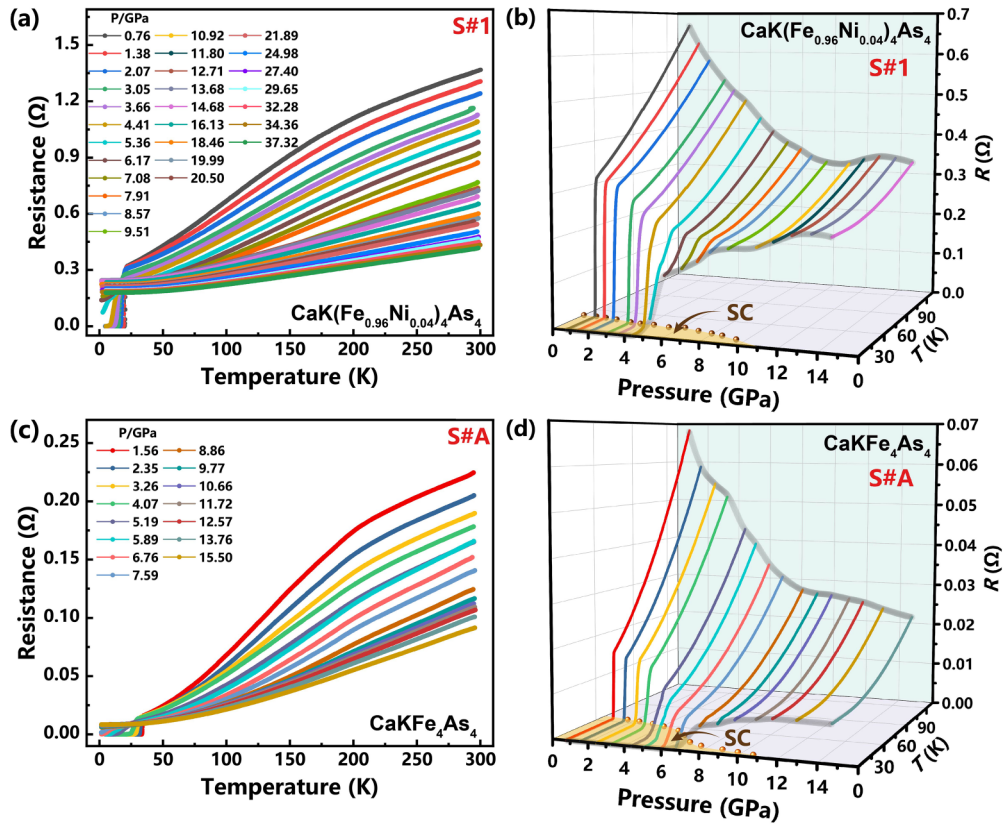


FIG. 1. The results of resistance measurements on the $\text{CaK}(\text{Fe}_{1-x}\text{Ni}_x)_4\text{As}_4$ ($x = 0.04$ and 0) at high pressures. (a) Temperature dependence of the resistance in the pressure range of 0.76 – 37.32 GPa for sample no. 1 of the $\text{CaK}(\text{Fe}_{0.96}\text{Ni}_{0.04})_4\text{As}_4$ single crystal. (b) Enlarged views of the resistance-temperature curves at different pressures for sample no. 1 of $\text{CaK}(\text{Fe}_{0.96}\text{Ni}_{0.04})_4\text{As}_4$. (c) Resistance as a function of temperature for pressures ranging from 1.56 to 15.5 GPa for sample no. A of the $\text{CaKFe}_4\text{As}_4$ single crystal. (d) Resistance-temperature curves at different pressures for sample no. A of $\text{CaKFe}_4\text{As}_4$.

Pressure tuning is an effective and clean way to manipulate the crystal and electronic structures without changing the chemistry, often providing significant information for understanding the underlying physics of the exotic state emerging from ambient pressure materials, through investigating the coevolution of electronic states and crystal structure. Some high-pressure studies on the $\text{AeAFe}_4\text{As}_4$ superconductors have been performed, and interesting results have been achieved from both experimental and theoretical sides [12–16,26], including the transition of bulk-to-percolating superconducting state [12], half-to-full collapse of the tetragonal phase [14,15,26]. These results provide the fundamental knowledge that the superconductivity and the lattice structure of these superconductors are intimately correlated and sensitive to the external pressure. However, the reported investigations of transport properties on Ni-doped and undoped $\text{CaKFe}_4\text{As}_4$ superconductors are performed under pressure below 6 GPa. What happens above 6 GPa remains unclear. In addition, the experimental evidence for the change of electronic state around the critical pressure of the half-collapse of the tetragonal (h-cT) phase is still lacking. In this paper, we perform the high-pressure studies on the doped and undoped samples up to the pressure where the superconductivity is fully suppressed and the f-cT phase forms.

High-quality single crystals of $\text{CaK}(\text{Fe}_{1-x}\text{Ni}_x)_4\text{As}_4$ ($x = 0.04$ and 0) were grown using the self-flux method [17,18,25].

The ambient-pressure values of T_c 's of the doped and undoped samples were determined to be 21 and 35 K, respectively, and the SVC transition for the $x = 0.04$ sample is about $T_N = 44$ K [24].

The high-pressure experimental methods can be found in the Supplemental Material (see Ref. [28]) and the pressure for all measurements was determined by the ruby fluorescence method [29]. We first performed temperature-dependent resistance measurements on the single crystal of $\text{CaK}(\text{Fe}_{0.96}\text{Ni}_{0.04})_4\text{As}_4$ in a DAC. To investigate the doping effect on the transport properties, a parallel measurement was conducted on the undoped $\text{CaKFe}_4\text{As}_4$ sample. As shown in Figs. 1(a) and 1(c), the superconductivity of both samples with and without the SVC state is sensitive to the pressure applied. For the sample with the SVC state, the ambient-pressure T_c is much lower than that of the sample without the SVC state. It shows that application of pressure renders T_c decreased, no matter whether they host the SVC state or not. Intriguingly, the superconductivity of these two samples is fully suppressed at almost the same critical pressure (~ 11 GPa) as shown in Figs. 1(b) and 1(d), suggesting that the initial SVC state has little influence on the critical pressure for destroying the superconducting state. We repeat the measurements with several new samples and obtain the reproducible results (see Ref. [28]). Moreover, we investigate the pressure effect on the onset transition temperature (T_N) of the SVC state for

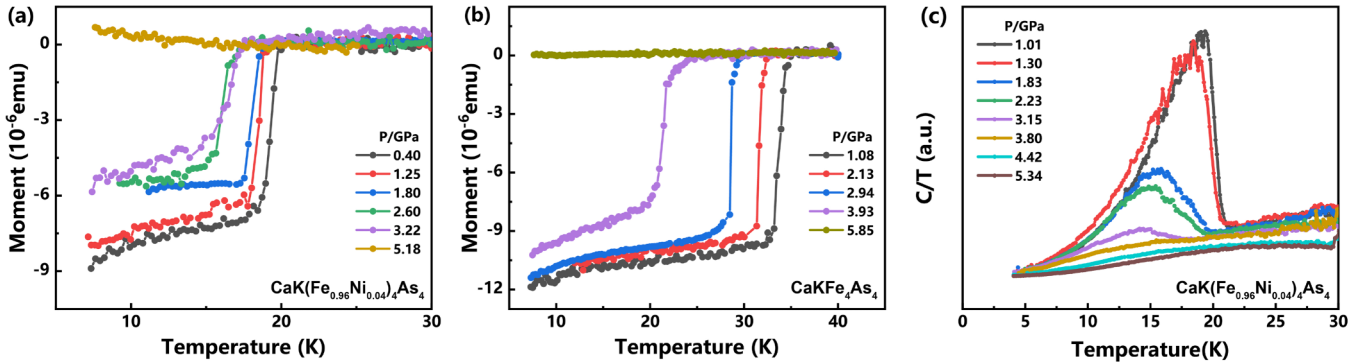


FIG. 2. The high-pressure results of the DC susceptibility and the heat capacity of the samples. (a) and (b) Magnetic moment as a function of temperature for the Ni-doped and undoped samples measured at different pressures. (c) The heat capacity versus temperature for the compressed $\text{CaK}(\text{Fe}_{0.96}\text{Ni}_{0.04})_4\text{As}_4$ sample.

our $\text{CaK}(\text{Fe}_{0.96}\text{Ni}_{0.04})_4\text{As}_4$ samples and find that T_N exhibits a monotonous decrease with the increment of pressure (see Ref. [28]), similar to what is observed in $\text{CaK}(\text{Fe}_{1-x}\text{Ni}_x)_4\text{As}_4$ ($x = 0.033$ and 0.05) and $\text{CaK}(\text{Fe}_{1-x}\text{Mn}_x)_4\text{As}_4$ ($x = 0.024$) samples [13,16].

It is noted that the previous studies showed that the superconductivity in the h-cT phase is not bulk [12]. To know more information about this issue, we performed high-pressure measurements of DC susceptibility for the doped and undoped samples [Figs. 2(a) and 2(b)], and the high-pressure heat-capacity measurements on the Ni-doped sample as well [Fig. 2(c)]. These results consistently demonstrate that the bulk superconductivity can be detected only in the ambient-pressure or low-pressure T phase.

To identify the similarity and peculiarity in the transport properties, superconductivity and the electronic state in $\text{CaK}(\text{Fe}_{0.96}\text{Ni}_{0.04})_4\text{As}_4$ and $\text{CaKFe}_4\text{As}_4$ samples, we performed high-pressure measurements on Hall resistance (R_{xy}) by sweeping the magnetic-field (H) applied perpendicular to the ab plane of the samples, from 0 to 6 T at 30 K for $\text{CaK}(\text{Fe}_{0.96}\text{Ni}_{0.04})_4\text{As}_4$ [Figs. 3(a) and 3(b)] and at 40 K for $\text{CaKFe}_4\text{As}_4$ [Figs. 3(c) and 3(d)]. We find that $R_{xy}(H)$ is positive below 2.4 GPa (the average value of the two independent runs $(2.33 + 2.46 \text{ GPa})/2 = 2.4 \text{ GPa}$) for the $\text{CaK}(\text{Fe}_{0.96}\text{Ni}_{0.04})_4\text{As}_4$ samples, and 3.88 GPa for the $\text{CaKFe}_4\text{As}_4$ samples (also the average value $-(3.90 + 3.85 \text{ GPa})/2 = 3.88 \text{ GPa}$). The method for determining the carriers' type of the investigated sample can be found in Ref. [28]. The plots of $R_{xy}(H)$ from our samples indicate that the role of hole-electron carriers is in a balanced state [$R_{xy}(H) = 0$] at a critical pressure (P_c) where the mobility should be close as well. Although the value of the P_c is different for the samples with and without the SVC state, the behavior of sign change in $R_H(P)$ is the same—below the P_c , the sample is dominated by hole carriers, whereas, above the P_c , the sample is dominated by electron carriers. The observation of the pressure-induced sign change of the Hall coefficient at the P_c provides important experimental evidence for the dramatic change of electronic structure—the reconstruction of the Fermi surface from a hole dominated to an electron dominated ones [30,31].

Since the structural stability is one of the key issues for understanding the phenomena found in the pressure range of our

experiments, we perform the high-pressure x-ray diffraction (XRD) measurements on the $\text{CaK}(\text{Fe}_{0.96}\text{Ni}_{0.04})_4\text{As}_4$ sample. The XRD patterns collected at different pressures are shown in Fig. 4(a). It is seen that all peaks measured under pressure up to 39.3 GPa can be well indexed by the tetragonal phase in the $P4/mmm$ space group, indicating that no structure phase transition occurs in the pressure range investigated. In Fig. 4(b), we illustrate the crystal structure of the $\text{CaK}(\text{Fe}_{0.96}\text{Ni}_{0.04})_4\text{As}_4$ sample and define the As ions adjacent to the Ca layers as As(1) and the K layers as As(2).

However, the lattice parameter a extracted from our XRD data shows an increase starting at $\sim 2.4 \text{ GPa}$ and reaching the maximum at $\sim 5 \text{ GPa}$, meanwhile, the lattice parameter c

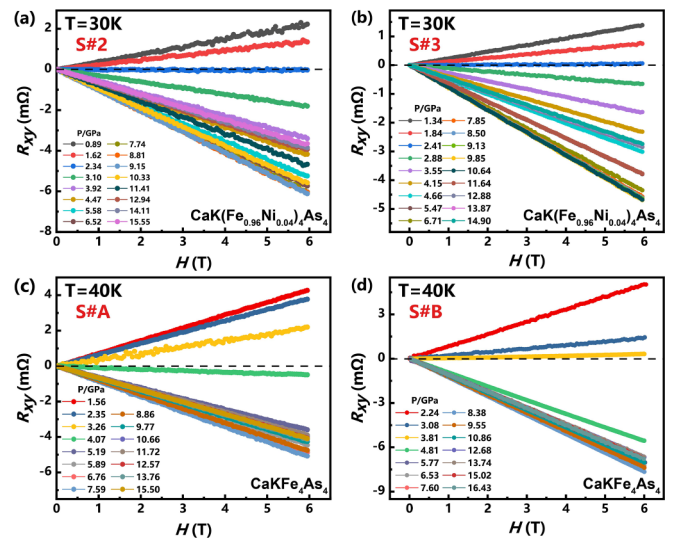


FIG. 3. Hall resistance (R_{xy}) as a function of magnetic-field (H) for the $\text{CaK}(\text{Fe}_{1-x}\text{Ni}_x)_4\text{As}_4$ ($x = 0.04$ and 0) single crystals. Plots of R_{xy} versus H for the $\text{CaK}(\text{Fe}_{0.96}\text{Ni}_{0.04})_4\text{As}_4$ single crystals measured at 30 K in the pressure range (a) 0.89–15.5 GPa, (b) 1.34–14.9 GPa. R_{xy} versus H for the $\text{CaKFe}_4\text{As}_4$ single crystals measured at 40 K in the pressure range (c) 1.56–15.5 GPa, (d) 2.24–16.43 GPa. The dashed line indicates $R_{xy}(B) = 0$ where the average pressures for samples no. 2 and no. 3 of the $\text{CaK}(\text{Fe}_{0.96}\text{Ni}_{0.04})_4\text{As}_4$ and sample no. A and no. B of the $\text{CaKFe}_4\text{As}_4$ single crystals are estimated to be ~ 2.4 and 3.88 GPa , respectively.

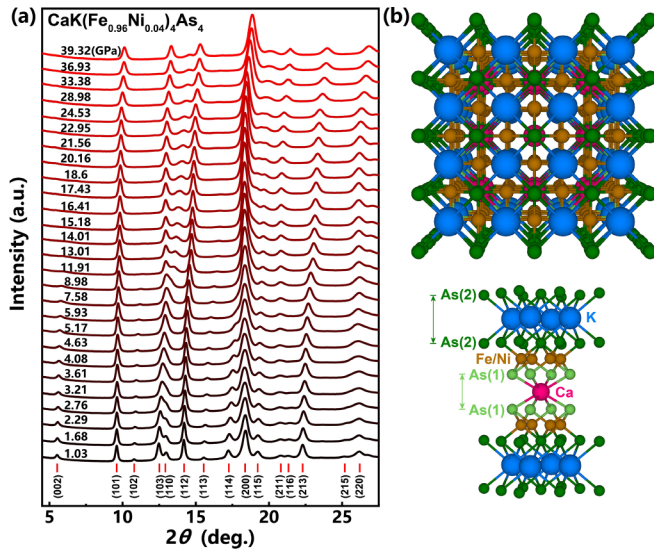


FIG. 4. X-ray diffraction results of the $\text{CaK}(\text{Fe}_{0.96}\text{Ni}_{0.04})_4\text{As}_4$ sample collected at high pressure and crystallographic illustration. (a) X-ray diffraction patterns measured at different pressures, showing no crystal structure phase transition in the experimental pressure range up to 39.32 GPa. (b) Schematic crystal structure of the $\text{CaK}(\text{Fe}_{0.96}\text{Ni}_{0.04})_4\text{As}_4$ sample.

displays a rapid decrease in this pressure range [Fig. 5(a)]. These results lead us to propose that the transition of the half-collapse of the tetragonal (h-cT) phase turns on and off at ~ 2.4 GPa and ~ 5 GPa, respectively. (Here, we define these critical pressures as P_{ch}^{on} and P_{ch}^{off}), and an intermedium phase composed of the initial tetragonal (T) phase and the partial h-cT phase exists in this pressure range. These results are similar to what have been observed in the pressurized $\text{CaKFe}_4\text{As}_4$ samples in which the lattice parameter a begins to increase at ~ 3.7 GPa and reaches a maximum at ~ 4.7 GPa [12]. Upon further compression to ~ 11 GPa, the second collapse occurs—the lattice parameter a and c also appear noticeable changes. (Here, we define this critical pressure as P_{cf}), implying that the T phase fully collapses (due to lack of more experimental information on the change in the f-cT phase, we are not able to identify the critical pressure that turns off the f-cT phase). The pressure-induced two collapses in the tetragonal $\text{CaK}(\text{Fe}_{0.96}\text{Ni}_{0.04})_4\text{As}_4$ sample are in accordance with the theoretical calculations and experimental results obtained from the measurements on the $\text{CaRbFe}_4\text{As}_4$ and $\text{Cs/RbEuFe}_4\text{As}_4$ samples [14,15,26].

We summarize our high-pressure results obtained from the measurements on $\text{CaK}(\text{Fe}_{0.96}\text{Ni}_{0.04})_4\text{As}_4$ in the pressure- T_c phase diagram [Fig. 5(b)]. The four distinct regions defined by the lattice structure can be seen in the diagram: (1) Low-pressure T phase region below P_{ch}^{on} in which the SVC state coexists with the SC state. When pressure is applied, both T_N and T_c decrease with increasing pressure until the pressure reaches to the P_{ch}^{on} . (2) An intermedium mixed phase region in which the T and h-cT phase coexist in the range of P_{ch}^{on} and P_{ch}^{off} . At the P_{ch}^{on} , the SVC state is entirely suppressed and the sample starts the transition from a T phase to h-cT phase [Fig. 5(a)]. Just at this pressure, the Hall coefficient (R_H) changes its sign from the positive to the neg-

ative [Fig. 5(c)]. These results demonstrate that the pressure drives a reconstruction of Fermi surface, which is associated with the transition from the T phase to the h-cT phase in a pressure range below ~ 5 GPa [Fig. 5(a)]. (3) The h-cT phase region lies in the range of P_{ch}^{off} and P_{cf} in which the T_c decreases continuously and disappears at the pressure of ~ 11 GPa. (4) The f-cT phase region above the critical pressure of P_{cf} in which the h-cT phase fully converts to the f-cT phase, and the corresponding electronic state of the h-cT phase is taken over by that of the nonsuperconducting f-cT phase.

To clarify the doping effect on the high-pressure behavior found in the sample with the SVC state, we compare its high-pressure experimental results with that measured from the undoped $\text{CaKFe}_4\text{As}_4$ sample. As shown in Figs. 5(d)–5(f), $\text{CaKFe}_4\text{As}_4$ bears the similar high-pressure behavior to that of $\text{CaK}(\text{Fe}_{0.96}\text{Ni}_{0.04})_4\text{As}_4$: T_c monotonically declines with the increment of pressure [Fig. 5(e)], in agreement with the results reported in Ref. [12]. At ~ 3.88 GPa (P_{ch}^{on}), the Hall coefficient (R_H) also displays a sign change from the positive to the negative, indicating that the ambient-pressure T phase of the sample begins its half collapse at this pressure [12,14]. A sudden increase in the lattice parameter a and the volume drop are also observed at ~ 3.7 GPa by Kaluarachchi *et al.* [12], very close to the P_{ch}^{on} determined by our Hall coefficient measurements [Fig. 5(f)]. Since the observed P_{ch}^{on} (~ 3.88 GPa) and P_{ch}^{off} (~ 4.9 GPa) by our Hall coefficient measurements is close to these (~ 3.7 and ~ 4.7 GPa) determined by the high pressure and low-temperature XRD measurements on the same sample [12], we define the pressures of 3.88 and 4.9 GPa as the P_{ch}^{on} and P_{ch}^{off} of our undoped sample. On further increasing pressure, T_c measured from both $\text{CaK}(\text{Fe}_{0.96}\text{Ni}_{0.04})_4\text{As}_4$ and $\text{CaKFe}_4\text{As}_4$ samples shows a monotonously decrease until the pressure around $P_{cf} = 11$ GPa [Figs. 5(b) and 5(e)], at the pressure of which doped- and undoped-samples undergo a transition from the h-cT phase to the f-cT phase [12,26] and lose their superconductivity. The observation of the pressure-induced SC-to-NSC transition and the identification on that the critical pressure of the SC-NSC transition coincide with the pressure of the lattice transition from the h-cT phase to the f-cT phase in the $\text{CaK}(\text{Fe}_{1-x}\text{Ni}_x)_4\text{As}_4$ ($x = 0.04$) superconductors.

Theoretical calculations on the undoped system find that the formation of the As(1)-As(1) bond across the Ca layers and the formation of the As(2)-As(2) bond across the K layer are responsible for the presence of the h-cT and the f-cT phases [12,26,32], and propose that the formed As-As bond weakens the Fe-As bonding [32–34], which, in turn, greatly affects the stability of superconductivity [32]. Our experimental results from the investigated $\text{CaK}(\text{Fe}_{1-x}\text{Ni}_x)_4\text{As}_4$ ($x = 0.04$ and 0) superconductors support this theoretical scenario, which implies that the stability of superconductivity in this kind of iron pnictides is closely associated with the state of the Fe-As bonding.

By comparing the high-pressure behavior of the $\text{CaK}(\text{Fe}_{0.96}\text{Ni}_{0.04})_4\text{As}_4$ and $\text{CaKFe}_4\text{As}_4$ samples, we find that the substitution of Ni on Fe site shifts the P_{ch}^{on} to lower pressure, while it has no obvious effects on the P_{ch}^{off} and the P_{cf} . Thus, understanding why the existence of the SVC state renders the P_{ch}^{on} to shift to lower pressure should be one of the key issues to reveal the underlying physics of the lattice

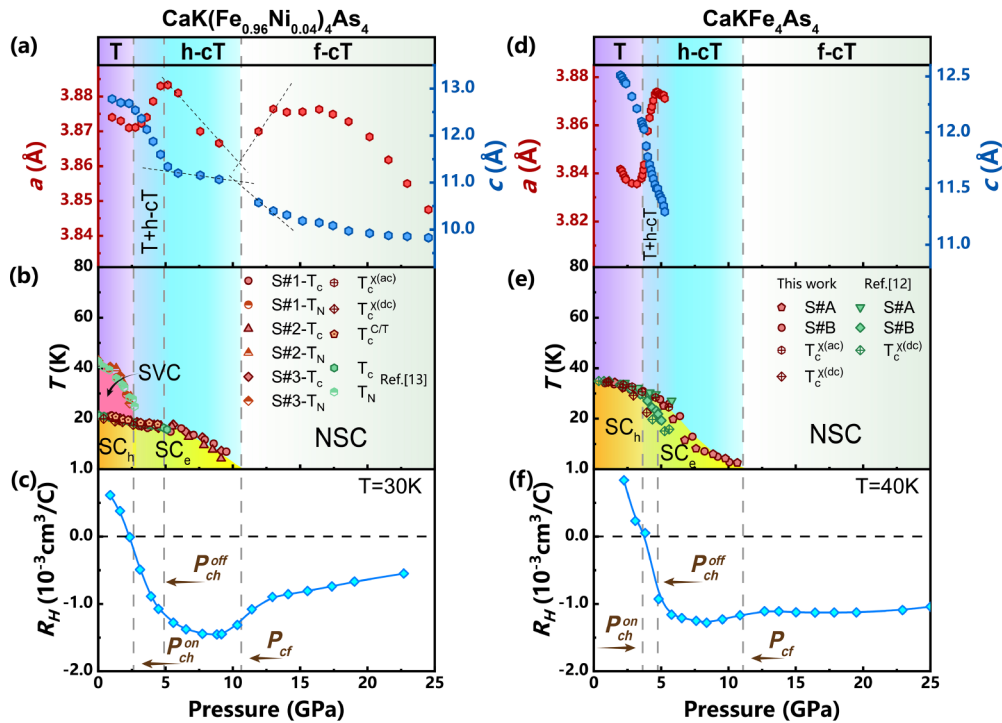


FIG. 5. Structure information, pressure-temperature phase diagram and Hall coefficient (R_H) of the $\text{CaK}(\text{Fe}_{1-x}\text{Ni}_x)_4\text{As}_4$ ($x = 0.04$ and 0) samples at different pressures. (a) and (d) Lattice parameters a and c versus pressure for the doped and undoped samples. (b) and (e) Pressure-temperature phase diagrams, displaying the evolution of the SVC, SC, and NSC states upon increasing pressure for the doped and undoped samples. (c) and (f) Pressure dependence of Hall coefficient (R_H) for the $\text{CaK}(\text{Fe}_{0.96}\text{Ni}_{0.04})_4\text{As}_4$ and $\text{CaKFe}_4\text{As}_4$ samples. T , h-cT, and f-cT represent the tetragonal phase, half-collapsed tetragonal phase, and full-collapsed tetragonal phase, respectively. T_N stands for the onset transition temperature of the SVC state. SC_h and SC_e represent the superconducting state with the dominance of hole carriers and the superconducting state with the dominance of electron carriers. The P_{ch}^{on} , P_{ch}^{off} represent the turn-on and turn-off pressures for the transition from the T phase to the h-cT phase. P_{cf} stands for the critical pressure for the transition from the h-cT phase to f-cT phase. The data in the (d) are taken from the Ref. [12]. For the $x = 0.04$ sample, $P_{ch}^{\text{on}} = 2.4$ GPa, $P_{ch}^{\text{off}} = 5$ GPa, and $P_{cf} = 11$ GPa, whereas, for the $x = 0$ sample, $P_{ch}^{\text{on}} = 3.88$ GPa, $P_{ch}^{\text{off}} = 4.9$ GPa, and $P_{cf} = 11$ GPa. $T_c^{\chi(\text{AC})}$, $T_c^{\chi(\text{DC})}$, and $T_c^{\chi/T}$ stand for the superconducting transition temperature obtained from the measurements of AC susceptibility, DC susceptibility and heat capacity, respectively.

half collapse. We propose that the left shift of the P_{ch}^{on} in the Ni-doped sample may be related to the interplay between the SVC state and the Fe-As hybridized state (the hybridization between the Fe $3d$ orbital and As $4p$ orbital electrons), which is an intriguing issue and deserves further investigations in the future. These results imply that the P_{ch}^{on} is sensitive to the existence of the competing order introduced by the chemical doping. Although the unchanged P_{ch}^{off} and P_{cf} is possibly related to the stability of the lattice that is still governed by the matrix of the initial T phase.

In conclusion, the coevolution of the SVC state, superconductivity, dominated carriers and stability of lattice structure in $\text{CaK}(\text{Fe}_{1-x}\text{Ni}_x)_4\text{As}_4$ ($x = 0.04$ and 0) superconductors has been investigated by the complementary measurements of high-pressure resistance, Hall coefficient and synchrotron x-ray diffraction in a wide pressure range involving superconducting to nonsuperconducting transition, and the corresponding half to full collapse of tetragonal phase transition. The three critical pressures are identified, through the comprehensive analysis of our results: P_{ch}^{on} and P_{ch}^{off} that are the turn-on and turn-off pressure of the h-cT phase transition, respectively, and P_{cf} that is the critical pressure of the f-cT

phase transition. Especially, we find that, in the transition from the T phase to the h-cT phase, R_H changes its sign from the positive to the negative, a manifestation for the reconstruction of the Fermi surface. These results achieved in this paper not only provide a consistent understanding on the results reported before, but also demonstrate the importance of the Fe-As bonding in stabilizing the superconductivity of the iron-pnictide superconductors through the “pressure window.”

This work was supported by the National Key Research and Development Program of China (Grants No. 2022YFA1403900, No. 2021YFA1401800, and No. 2018YFA0704200), the National Natural Science Foundation of China (Grants No. U2032214, No. 12104487, No. 12122414, No. 12004419, and No. 11961160699), and the Strategic Priority Research Program (B) of the Chinese Academy of Sciences (Grant No. XDB25000000). J.G., S.C., and H. L. are grateful for support from the Youth Innovation Promotion Association of the Chinese Academy of Sciences (Grants No. 2019008 and No. Y202001) and the China Postdoctoral Science Foundation (Grant No. E0BK111).

- [1] Y. Kamihara, T. Watanabe, M. Hirano, and H. Hosono, Iron-based layered superconductor $\text{La}[\text{O}_{1-x}\text{F}_x]\text{FeAs}$ ($x = 0.05-0.12$) with $T_c = 26$ K, *J. Am. Chem. Soc.* **130**, 3296 (2008).
- [2] F. C. Hsu, J. Y. Luo, K. W. Yeh, T. K. Chen, T. W. Huang, P. M. Wu, Y. C. Lee, Y. L. Huang, Y. Y. Chu, D. C. Yan *et al.*, Superconductivity in the PbO-type structure α -FeSe, *Proc. Natl. Acad. Sci. USA* **105**, 14262 (2008).
- [3] C. W. Chu, L. Z. Deng, and B. Lv, Hole-doped cuprate high temperature superconductors, *Physica C* **514**, 290 (2015).
- [4] B. Keimer, S. A. Kivelson, M. R. Norman, S. Uchida, and J. Zaanen, From quantum matter to high-temperature superconductivity in copper oxides, *Nature (London)* **518**, 179 (2015).
- [5] J. Zaanen, Superconducting electrons go missing, *Nature (London)* **536**, 282 (2016).
- [6] M. Rotter, M. Tegel, and D. Johrendt, Superconductivity at 38 K in the Iron Arsenide $(\text{Ba}_{1-x}\text{K}_x)\text{Fe}_2\text{As}_2$, *Phys. Rev. Lett.* **101**, 107006 (2008).
- [7] X. C. Wang, Q. Q. Liu, Y. X. Lv, W. B. Gao, L. X. Yang, R. C. Yu, F. Y. Li, and C. Q. Jin, The superconductivity at 18 K in LiFeAs system, *Solid State Commun.* **148**, 538 (2008).
- [8] X. Zhu, F. Han, G. Mu, P. Cheng, B. Shen, B. Zeng, and H. H. Wen, Transition of stoichiometric $\text{Sr}_2\text{VO}_3\text{FeAsO}$ to a superconducting state at 37.2 K, *Phys. Rev. B* **79**, 220512(R) (2009).
- [9] N. Ni, J. M. Allred, B. C. Chan, and R. J. Cava, High T_c electron doped $\text{Ca}_{10}(\text{Pt}_3\text{As}_8)(\text{Fe}_2\text{As}_2)_5$ and $\text{Ca}_{10}(\text{Pt}_4\text{As}_8)(\text{Fe}_2\text{As}_2)_5$ superconductors with skutterudite intermediary layers, *Proc. Natl. Acad. Sci. USA* **108**, E1019 (2011).
- [10] A. Iyo, K. Kawashima, T. Kinjo, T. Nishio, S. Ishida, H. Fujihisa, Y. Gotoh, K. Kihou, H. Eisaki, and Y. Yoshida, New-Structure-Type Fe-Based Superconductors: $\text{CaAFe}_4\text{As}_4$ ($A = \text{K}, \text{Rb}, \text{Cs}$) and $\text{SrAFe}_4\text{As}_4$ ($A = \text{Rb}, \text{Cs}$), *J. Am. Chem. Soc.* **138**, 3410 (2016).
- [11] W. R. Meier, T. Kong, U. S. Kaluarachchi, V. Taufour, N. H. Jo, G. Drachuck, A. E. Böhmer, S. M. Saunders, A. Sapkota, A. Kreyssig *et al.*, Anisotropic thermodynamic and transport properties of single-crystalline $\text{CaKFe}_4\text{As}_4$, *Phys. Rev. B* **94**, 064501 (2016).
- [12] U. S. Kaluarachchi, V. Taufour, A. Sapkota, V. Borisov, T. Kong, W. R. Meier, K. Kothapalli, B. G. Ueland, A. Kreyssig, R. Valentí *et al.*, Pressure-induced half-collapsed-tetragonal phase in $\text{CaKFe}_4\text{As}_4$, *Phys. Rev. B* **96**, 140501(R) (2017).
- [13] L. Xiang, W. R. Meier, M. Xu, U. S. Kaluarachchi, S. L. Bud'ko, and P. C. Canfield, Pressure-temperature phase diagrams of $\text{CaK}(\text{Fe}_{1-x}\text{Ni}_x)_4\text{As}_4$ superconductors, *Phys. Rev. B* **97**, 174517(R) (2018).
- [14] R. L. Stillwell, X. Wang, L. Wang, D. J. Campbell, J. Paglione, S. T. Weir, Y. K. Vohra, and J. R. Jeffries, Observation of two collapsed phases in $\text{CaRbFe}_4\text{As}_4$, *Phys. Rev. B* **100**, 045152 (2019).
- [15] D. E. Jackson, D. VanGennep, W. Bi, D. Zhang, P. Materne, Y. Liu, G.-H. Cao, S. T. Weir, Y. K. Vohra, and J. J. Hamlin, Superconducting and magnetic phase diagram of $\text{RbEuFe}_4\text{As}_4$ and $\text{CsEuFe}_4\text{As}_4$ at high pressure, *Phys. Rev. B* **98**, 014518 (2018).
- [16] L. Xiang, M. Xu, S. L. Bud'ko, and P. C. Canfield, Pressure-temperature phase diagram of $\text{CaK}(\text{Fe}_{1-x}\text{Mn}_x)_4\text{As}_4$ ($x = 0.024$), *Phys. Rev. B* **106**, 134505 (2022).
- [17] C. Liu, P. Bourges, Y. Sidis, T. Xie, G. He, F. Bourdarot, S. Danilkin, H. Ghosh, S. Ghosh, X. Ma *et al.*, Preferred Spin Excitations in the Bilayer Iron-Based Superconductor $\text{CaK}(\text{Fe}_{0.96}\text{Ni}_{0.04})_4\text{As}_4$ with Spin-Vortex Crystal Order, *Phys. Rev. Lett.* **128**, 137003 (2022).
- [18] T. Xie, Y. Wei, D. Gong, T. Fennell, U. Stuhr, R. Kajimoto, K. Ikeuchi, S. Li, J. Hu, and H. Luo, Odd and Even Modes of Neutron Spin Resonance in the Bilayer Iron-Based Superconductor $\text{CaKFe}_4\text{As}_4$, *Phys. Rev. Lett.* **120**, 267003 (2018).
- [19] T. Xie, C. Liu, F. Bourdarot, L.-P. Regnault, S. Li, and H. Luo, Spin-excitation anisotropy in the bilayer iron-based superconductor $\text{CaKFe}_4\text{As}_4$, *Phys. Rev. Res.* **2**, 022018(R) (2020).
- [20] B. Q. Song, M. Xu, V. Borisov, O. Palasyuk, C. Z. Wang, R. Valentí, P. C. Canfield, and K. M. Ho, Construction of A-B heterolayer intermetallic crystals: Case studies of the 1144-phase TM-phosphides $\text{AB}(\text{TM})_4\text{P}_4$ ($\text{TM} = \text{Fe}, \text{Ru}, \text{Co}, \text{Ni}$), *Phys. Rev. Mater.* **5**, 094802 (2021).
- [21] W. Liu, L. Cao, S. Zhu, L. Kong, G. Wang, M. Papaj, P. Zhang, Y.-B. Liu, H. Chen, G. Li *et al.*, A new Majorana platform in an Fe-As bilayer superconductor, *Nat. Commun.* **11**, 5688 (2020).
- [22] A. Kreyssig, J. M. Wilde, A. E. Böhmer, W. Tian, W. R. Meier, B. Li, B. G. Ueland, M. Xu, S. L. Bud'ko, P. C. Canfield *et al.*, Antiferromagnetic order in $\text{CaK}(\text{Fe}_{1-x}\text{Ni}_x)_4\text{As}_4$ and its interplay with superconductivity, *Phys. Rev. B* **97**, 224521 (2018).
- [23] S. L. Bud'ko, V. G. Kogan, R. Prozorov, W. R. Meier, M. Xu, and P. C. Canfield, Coexistence of superconductivity and magnetism in $\text{CaK}(\text{Fe}_{1-x}\text{Ni}_x)_4\text{As}_4$ as probed by ^{57}Fe Mössbauer spectroscopy, *Phys. Rev. B* **98**, 144520 (2018).
- [24] W. R. Meier, Q. P. Ding, A. Kreyssig, S. L. Bud'ko, A. Sapkota, K. Kothapalli, V. Borisov, R. Valentí, C. D. Batista, P. P. Orth *et al.*, Hedgehog spin-vortex crystal stabilized in a hole-doped iron-based superconductor, *npj Quantum Mater.* **3**, 5 (2018).
- [25] R. Yang, Y. Dai, B. Xu, W. Zhang, Z. Qiu, Q. Sui, C. C. Homes, and X. Qiu, Anomalous phonon behavior in superconducting $\text{CaKFe}_4\text{As}_4$: An optical study, *Phys. Rev. B* **95**, 064506 (2017).
- [26] V. Borisov, P. C. Canfield, and R. Valentí, Trends in pressure-induced layer-selective half-collapsed tetragonal phases in the iron-based superconductor family $\text{AeAFe}_4\text{As}_4$, *Phys. Rev. B* **98**, 064104 (2018).
- [27] S. Pailhes, Y. Sidis, P. Bourges, C. Ulrich, V. Hinkov, L. P. Regnault, A. Ivanov, B. Liang, C. T. Lin, C. Bernhard *et al.*, Two Resonant Magnetic Modes in an Overdoped High T_c Superconductor, *Phys. Rev. Lett.* **91**, 237002 (2003).
- [28] See Supplemental Material at <http://link.aps.org/supplemental/10.1103/PhysRevB.108.054415> for the experimental method and extended data for $\text{CaK}(\text{Fe}_{1-x}\text{Ni}_x)_4\text{As}_4$ ($x = 0.04$ and 0); also see Refs. [12,13,17,24].
- [29] H. K. Mao, J. Xu, and P. M. Bell, Calibration of the ruby pressure gauge to 800 kbar under quasi-hydrostatic conditions, *Geophys. Res. Solid Earth Planets* **91**, 4673 (1986).
- [30] G. Lin, J. Guo, Y. Zhu, S. Cai, Y. Zhou, C. Huang, C. Yang, S. Long, Q. Wu, Z. Mao *et al.*, Correlation between Fermi surface reconstruction and superconductivity in pressurized $\text{FeTe}_{0.55}\text{Se}_{0.45}$, *Phys. Rev. B* **101**, 214525 (2020).
- [31] D. Kang, Y. Zhou, W. Yi, C. Yang, J. Guo, Y. Shi, S. Zhang, Z. Wang, C. Zhang, S. Jiang *et al.*, Superconductivity emerging from a suppressed large magnetoresistant state in tungsten ditelluride, *Nat. Commun.* **6**, 7804 (2015).

- [32] R. Yang, C. Le, L. Zhang, B. Xu, W. Zhang, K. Nadeem, H. Xiao, J. Hu, and X. Qiu, Formation of As-As bond and its effect on absence of superconductivity in the collapsed tetragonal phase of $\text{Ca}_{0.86}\text{Pr}_{0.14}\text{Fe}_2\text{As}_2$: An optical spectroscopy study, *Phys. Rev. B* **91**, 224507 (2015).
- [33] T. Yildirim, Strong Coupling of the Fe-Spin State and the As-As Hybridization in Iron-Pnictide Superconductors from First-Principle Calculations, *Phys. Rev. Lett.* **102**, 037003 (2009).
- [34] J. Diehl, S. Backes, D. Guterding, H. O. Jeschke, and R. Valentí, Correlation effects in the tetragonal and collapsed-tetragonal phase of CaFe_2As_2 , *Phys. Rev. B* **90**, 085110 (2014).